Earth and Planetary Science Letters 434 (2016) 112–116

Contents lists available at ScienceDirect

Earth and Planetary Science Letters

www.elsevier.com/locate/epsl

Atmospheric resonant oscillations by the 2014 eruption of the Kelud volcano, Indonesia, observed with the ionospheric total electron contents and seismic signals

Yuki Nakashima [a,*], Kosuke Heki [a], Akiko Takeo [a,b], Mokhamad N. Cahyadi [c], Arif Aditiya [d], Kazunori Yoshizawa [a]

[a] Department of Natural History Sciences, Hokkaido University, N10, W8, Kita-ku, Sapporo 060 0810, Japan
[b] Earthquake Research Institute, The University of Tokyo, 1-1-1 Yayoi, Bunkyo-ku, Tokyo, Japan
[c] Geomatics Engineering Institut Teknologi Sepuluh Nopember (ITS), Surabaya, Indonesia
[d] Badan Informasi Geospasial, Jl. Raya Jakarta, Bogor KM. 46, Cibinong, Jawa Barat, Indonesia

ARTICLE INFO

Article history:
Received 6 July 2015
Received in revised form 12 November 2015
Accepted 19 November 2015
Available online 4 December 2015
Editor: P. Shearer

Keywords:
GNSS
TEC
ionosphere
atmospheric free oscillation
acoustic wave
broadband seismometer

ABSTRACT

Acoustic waves from volcanic eruptions are often observed as infrasound in near fields. Part of them propagate upward and disturb the ionosphere, and can be observed with Total Electron Content (TEC) data from Global Navigation Satellite System (GNSS) receivers. Here we report TEC variations after the 13 February 2014 Plinian eruption of the Kelud volcano, East Java, Indonesia, observed with regional GNSS networks. Significant disturbances in TEC were detected with six GNSS satellites, and wavelet analysis showed that harmonic oscillations started at ~16:25 UT and continued for ~2.5 h. The amplitude spectrum of the TEC time series showed peaks at 3.7 mHz, 4.8 mHz and 6.8 mHz. Long-wavelength standing waves with a wide range of wavelength trapped in the lower atmosphere are excited by the Plinian eruption. Amplitude spectra of the ground motion recorded by seismometers, however, had frequency components at discrete wave-periods. The condition for the resonant oscillations between the atmosphere and the solid Earth is satisfied only at these discrete wave-period and horizontal wavelength pairs, therefore efficient energy transfer from the atmospheric standing waves to the solid Earth Rayleigh waves occurred at discrete periods and resulted in the harmonic ground motion.

1. Introduction

Large volcanic eruptions often disturb the upper atmosphere including the ionosphere of the earth. Such disturbances can be observed by GNSS receivers as changes in TEC. For example, an N-shaped change in TEC, lasting for ~100 s, was found after the 2004 September Vulcanian explosion of the Asama volcano, central Japan (Heki, 2006). Such disturbances are caused by compressional pulse in the neutral atmosphere propagating upward as an acoustic wave. A longer-lasting volcanic eruption often show a different type of atmospheric disturbances. For example, Dautermann et al. (2009b) detected ionospheric disturbances excited by the eruption of the Soufriere Hills volcano, the Lesser Antilles, in 2003. They included 1.4 mHz internal gravity wave and ~4 mHz atmospheric eigenfrequency components. Dautermann et al. (2009a) investigated the strain gauge records after this eruption, and also found the ~4 mHz oscillation in the solid earth.

Such resonant oscillations of the lower atmosphere are also observed by GNSS-TEC after large earthquakes. Choosakul et al. (2009) reported that the 2004 Sumatra–Andaman earthquake excited ~4 mHz oscillation in the ionospheric lasting for hours. Rolland et al. (2011) analyzed various types of ionospheric perturbations by the 2011 Tohoku-oki earthquake. It includes an N-shaped wave excited by the Rayleigh wave, and the 3.7 mHz and 4.4 mHz acoustic-trap-modes excited in the lower atmosphere and leaked into the ionosphere. Then, the internal gravity wave appeared ~45 min later and propagated concentrically outward by ~225 m/s from the epicenter. Saito et al. (2011) detected 3.7 mHz, 4.5 mHz and 5.3 mHz frequency peaks in the TEC changes. Nishioka et al. (2013) reported internal gravity waves and lower atmospheric trapped waves excited by the 2013 moore EF5 tornado.

Atmospheric resonant oscillations also excite secondary oscillations in the solid Earth, and their frequencies are explained by the

* Corresponding author.
E-mail address: nakashima0124@frontier.hokudai.ac.jp (Y. Nakashima).

http://dx.doi.org/10.1016/j.epsl.2015.11.029
0012-821X/

normal mode theory (Lognonné et al., 1998). The Rayleigh waves in very long period seismograms, after the 1991 Pinatubo eruption, had two peaks, which are interpreted as coupling between the atmospheric oscillations excited by the volcanic eruption and the Rayleigh wave (Kanamori and Mori, 1992). Widmer and Zürn (1992) also reported vertical oscillations of the ground observed by gravimeters around the world. Later, Kanamori et al. (1994) proposed physical mechanisms of such oscillations, but the ground motion period is underestimated about 10%.

Watada and Kanamori (2010) provided an excitation mechanism; the fundamental and overtone of the atmospheric long-wavelength acoustic waves trapped in the low-sound velocity channel in the atmosphere below the thermosphere, and the fundamental mode which propagated as Rayleigh waves in the solid Earth share the same horizontal wavelength along the ground surface and the same wave periods. This acoustic resonance between the atmosphere and the solid Earth resulted in the observed harmonic ground motion composed of Rayleigh waves at two resonance periods. They employed the normal mode method for a combined Earth model with the solid Earth, the ocean and the atmosphere up to 200 km altitude, and succeeded in re-producing as a normal mode summation the harmonic ground motion excited by a point source that models a volcanic eruption in the atmosphere.

In this paper, we report preliminary observation results of harmonic oscillations in ionospheric TEC and seismic records after the 2014 February Plinian eruption of the Kelud volcano, eastern Java, Indonesia. The Kelud volcano is a very explosive volcano, and has erupted 8 times for the last one hundred years. The 2014 February eruption fractured the lava dome made by the 2007 eruption and created a new crater (Sulaksana et al., 2014). Corentin et al. (2015) interpreted the eruption sequence from infrasound and seismic observations. The oscillation in the ionosphere and lithosphere would have been caused by the lower atmospheric trapped waves excited by this eruption. We compare the results from the two kinds of sensors, and discuss how the 13 February 2014 Kelud volcano eruption excited these atmospheric trapped waves, from the oscillations observed in the ionosphere and the solid Earth.

2. Data analysis and results

2.1. GNSS-TEC data

Ionospheric delays of microwave signals from GNSS satellites are frequency dependent, and phase differences between the L1 and L2 carriers provide information on the ionosphere between the satellite and the ground station. TEC is the number of electrons integrated along the line-of-sight, and can be calculated from the L1 and L2 phase differences. We extracted the TEC information before and after the 2014 February eruption of the Kelud volcano from the raw data of 37 GNSS stations in and around Indonesia. The observation data are from three networks, (1) the GNSS network in Java run by the Badan Informasi Geospasial (BIG), (2) Sumatra GPS Array (SuGAr) operated in Sumatra by Indonesian Institute of Science and California Institute of Technology, and (3) International GNSS Service (IGS) stations (Fig. 1). The SuGAr stations observed only Global Positioning System (GPS), the American GNSS, every 15 s. Other stations received signals from both GPS and GLONASS (GLObal'naya NAvigatsionnaya Sputnikovaya Sistema), the Russian GNSS, every 30 s, except for COCO where only GPS data are recorded.

We extracted the components with periods around 270 s from slant TEC time series using the Mexican-hat wavelet. In order to make it possible to compare amplitudes between different station–satellite pairs, we converted the amplitudes into those in vertical

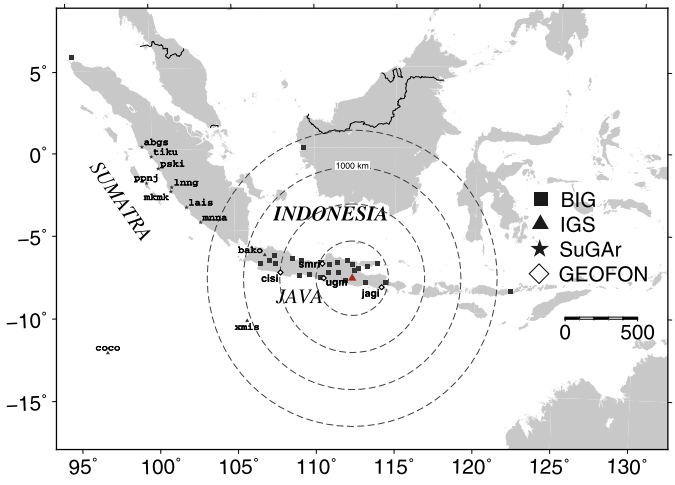

Fig. 1. Map of the Java Island and nearby islands, and the GNSS stations and broadband seismometers used in this study. The Kelud volcano is marked with the red triangle in Eastern Java Island. Black triangles and stars indicate IGS and SuGAR stations, respectively. We use also 26 stations which are run by BIG. White diamonds show GEOFON stations whose waveforms are shown in Figs. 3 and 4. (For interpretation of the references to color in this figure legend, the reader is referred to the web version of this article.)

TEC by multiplying with the cosine of the incidence angle of the line-of-sight with a thin layer at 250 km height. This height is also used to calculate the coordinates of sub-ionospheric points (SIPs).

After extracting the 270 s components, we estimated their propagation velocity by plotting the time and distance from the volcano of the TEC disturbances following Rolland et al. (2011). The estimated propagation velocity was ∼0.8 km/s, close to the acoustic wave speed in the F region of the ionosphere, and the oscillation in this period continued from 16:25 UT to 19:00 UT (Fig. 2). The SIPs of the disturbance in this frequency show clear concentric wavefronts propagating outward from the volcano (Fig. 2(c), Animation S1).

We obtained the frequency spectrum of the TEC oscillations. First, we extracted components with frequencies 2.0–8.0 mHz with a band-pass filter for the stations within 1000 km from the volcano. At first, for individual satellites, we adjusted the time axes of the time series of different stations assuming 0.8 km/s as the propagation velocity. The TEC data obtained with the same satellite results have similar geometry, and geometry plays an important role in TEC observations. We confirmed that these waveforms have similar structure, and then we further stacked them again (Fig. 3(a)), and then converted the doubly-stacked time series into the frequency domain. The spectrum showed two clear peaks at 3.7 mHz and 4.8 mHz (Fig. 3(a)).

2.2. Seismic data

The 2014 eruption of the Kelud volcano was a very explosive one and it caused many solid Earth and atmospheric events which destroyed observation instruments near the volcano. Corentin et al. (2015) investigated the eruption sequence with remote (>200 km) low-frequency-seismic (<0.2 Hz) and infrasound data. They found three types of seismic signal (S_LL: long lasting wave, S_P1: only visible nearby sites and S_P2: short-duration energetic signal) and two types of infrasound signal (I_1: first event and I_LL: long lasting second event) and constructed the eruption sequence from difference of these signals. Here we also look into the eruption time-line from the seismometer records of periods 17–33 s observed at three stations with the STS-2 broadband sensors of GEOFON ∼200 km from the volcano, and another GEOFON station ∼500 km from the volcano (Fig. 4). The signal first appears at

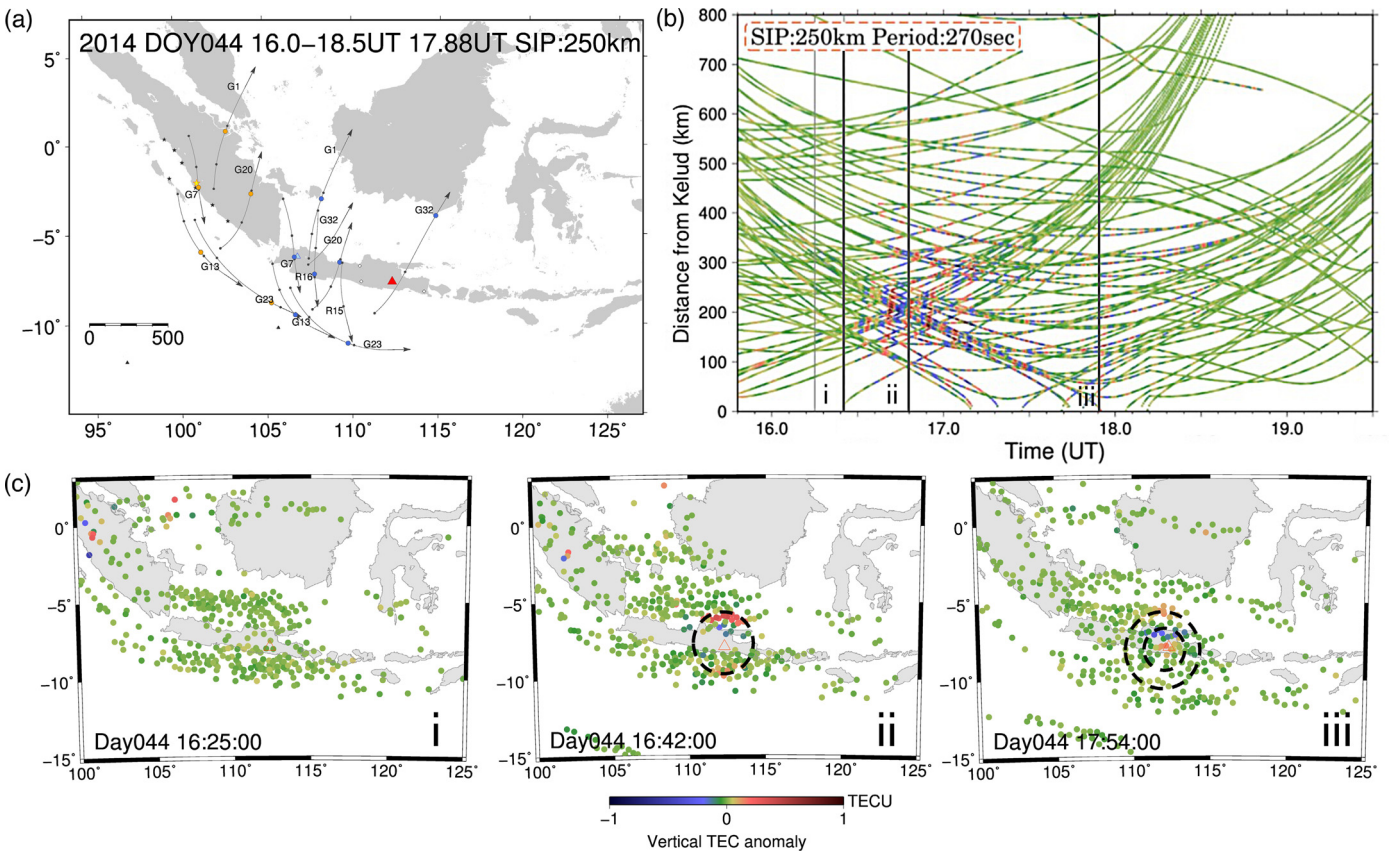

Fig. 2. (a) Trajectories of SIP of the GNSS stations viewed from LNNG and BAKO GNSS stations. The red triangle indicates the Kelud volcano. Large and small circles on the SIP tracks indicate SIPs at 17:53 UT and at 16:00, 17:00 and 18:00, respectively. (b) The horizontal and the vertical axes show time in UT and distance from the Kelud volcano, respectively. Colors indicate amplitudes of the component with the period of 270 s extracted by wavelet transform. (c) Spatial distributions of the 270 s component TEC oscillations at three time epochs, (i) 16:25 UT (ii) 16:42 UT (iii) 17:54 UT. (For interpretation of the references to color in this figure legend, the reader is referred to the web version of this article.)

around 16 UT at the stations ~200 km from the volcano. The seismic records include both Rayleigh waves and ground motion due to acoustic waves (e.g., Corentin et al., 2015). For distinguishing between these waves, we used the difference in i) the propagation velocity, and ii) the phase shifts between horizontal and vertical components (Fig. S1). The first signal could be then interpreted as the ground motion due to an acoustic wave (i.e. not a wave in the solid earth) that was excited at ~15:46 UT at the volcano, and propagated outward in the lower atmosphere with the speed of ~0.3 km/s. Tremor starting at 16:12 UT would also be of acoustic origin, and would have started at ~16:01 UT at the volcano. It continued for more than one hour. In addition, a relatively large amplitude wave packet propagating with the Rayleigh wave speed, ~4 km/s, seems to have been excited at the volcano at ~16:14 UT. From these seismic records, we interpreted that the initial explosion occurred at 15:46, which was followed by the start of the Plinian eruption ~15 min later. Then, an unknown event occurred at ~16:14 UT that generated the Rayleigh wave in the solid earth.

In Fig. 3(b), we decomposed seismic records at UGM, located ~200 km west from the volcano, into three bands of periods, i.e. 17–33 s, 100–200 s and 200–333 s. We interpret that the long-lasting ground oscillation in the long-period band includes the resonant ground motion coupled to the acoustic resonance in the lower atmosphere. Components with periods longer than 100 s started at 16:25, which is different from the initiation at 16:01 at shorter periods. It might be reflecting an increase of volcanic activity due to an event in the solid earth at 16:14 such as the dome collapse or the vent expansion. Components with periods of 17–33 s or 100–200 s terminated at ~18:00 UT, which possibly reflect the end of the Plinian eruption. On the other hand, the oscillations with periods of 200–333 s continued until ~19:00 UT. Because this period band includes those of the ionospheric oscillations, these oscillations would have been excited by the atmospheric free oscillation that continued ~1 h after the termination of the Plinian eruption.

Seismic signals with periods of 100–1000 s were observed at the 78 broadband seismometers (STS-1) of the Global Seismic Network (GSN) around the world (Fig. S2). The signal is shown to come from the Kelud volcano (Fig. S3) with the speed of the fundamental-mode Rayleigh wave (Fig. S4) for the Preliminary Reference Earth Model (PREM) by Dziewonski and Anderson (1981). Assuming the Rayleigh wave phase velocity, we estimated the source time function at the Kelud volcano by stacking velocity waveforms after the corrections of sensor responses (Fig. 3(b)). The spectrum shows broad source with several clear peaks including those at 3.7 mHz, 4.8 mHz, 5.7 mHz and 6.8 mHz (Fig. 3(b)). If we assume atmospheric top free surface boundary is ~90 km above ground, the eigenfrequencies of the standing acoustic modes in the atmospheric layer are 3.7, 4.7, 5.8 and 7.1 mHz for fundamental, first, second, third and fourth overtones in the vertical direction, respectively (Watada and Kanamori, 2010). The altitude of the thermopause (~100 km) calculated from the International Reference Ionosphere (IRI) (Bilitza et al., 2011) is close to this assumption. The continuous spectrum would reflect the turbulent atmospheric waves excited directly by the Plinian eruption. The discrete amplitude peaks are explained by the resonant oscillation of the lower atmosphere and its leakage into the solid Earth as demonstrated by Watada and Kanamori (2010).

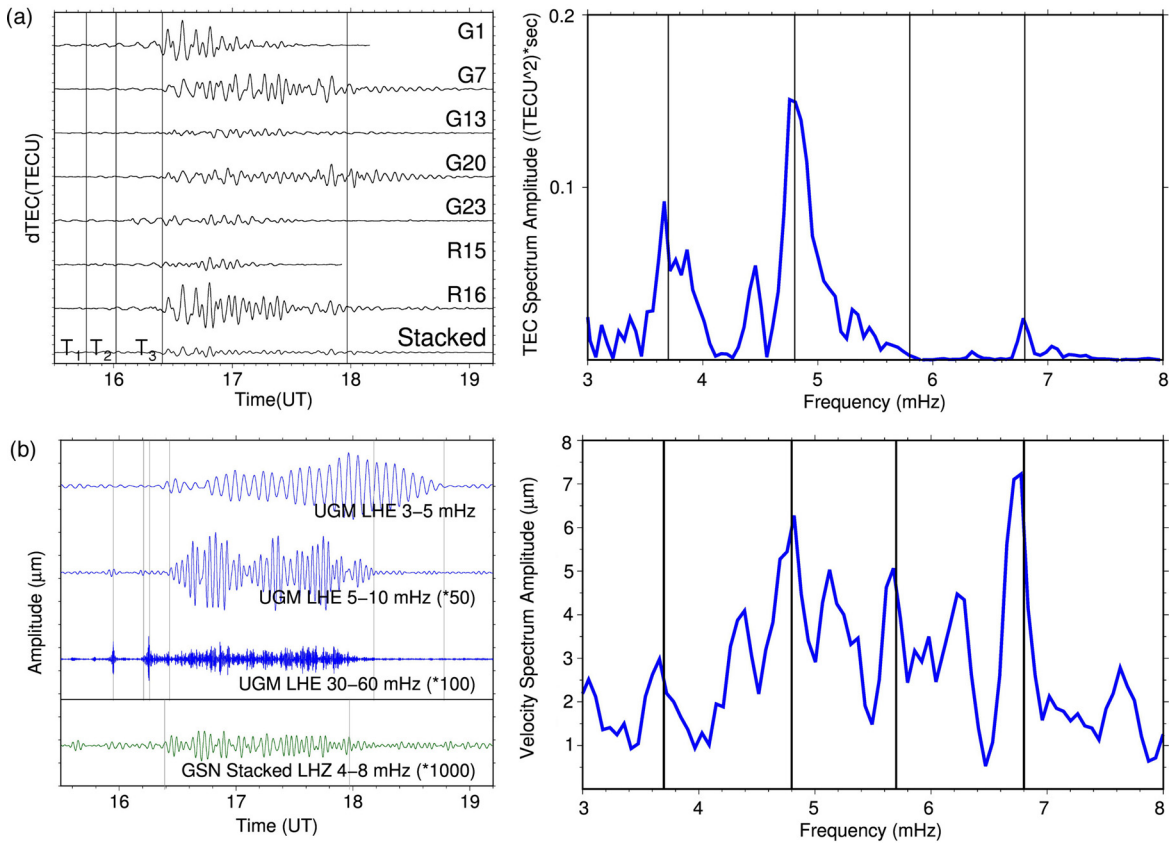

Fig. 3. (a) The left panel shows the TEC changes observed by seven GNSS satellites, five GPS (1, 7, 13, 20, 23) and two GLONASS satellites (15, 16). Vertical lines show events indicated in Fig. 4. Time series of multiple sites are reduced to those at the source of the disturbance (i.e. the Kelud volcano) by adjusting the time axes assuming the propagation velocity of 0.8 km/s backward the SIPs. These seven time series are stacked to produce one time series at the bottom, whose frequency spectrum is given in the right panel. Gray vertical lines show 3.7 mHz, 4.8 mHz, 5.7 mHz and 6.8 mHz. (b) Blue curves in the left panel show vertical velocity waveforms at the UGM station (200 km from the Kelud) with periods of 200–333 s (top), 100–200 s (middle) and 17–33 s (bottom). These waves are detected by a STS-2 seismometer as ground motion excited by the lower atmosphere. The green curve indicates the source time function calculated from vertical velocity waveforms of 72 STS-1 seismometers of the Global Seismic Network. It shows Rayleigh waves propagating in the solid earth. Vertical lines show events indicated in Fig. 4. The frequency spectrum of the source time function is shown in the right panel. Gray vertical lines are the same as panels (a). (For interpretation of the references to color in this figure legend, the reader is referred to the web version of this article.)

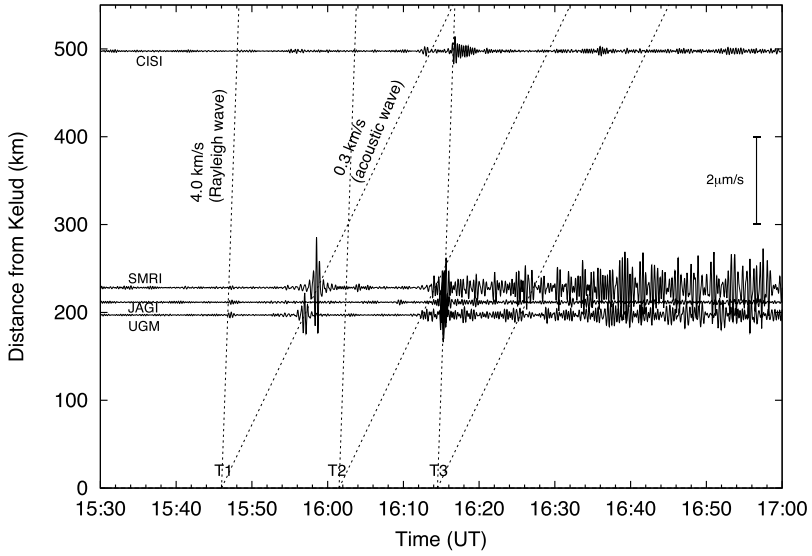

Fig. 4. Waveforms observed at 4 GEOFON seismic stations on 13 February 2014. Vertical components of the raw records at a band-pass filter of 17–33 s are plotted. Dashed lines show gradients corresponding to propagation speeds of 0.3 km/s and 4.0 km/s. The signal appearing around 16:00 would be the acoustic wave signal excited at T1=15:46:00 and propagated from the Kelud volcano. The continuous tremor, also of acoustic wave origin, would have started at T2=16:01:30, and lasted for hours. We can also see the wave packet at T3=16:14:30 propagating with the Rayleigh wave speed of ∼4.0 km/s.

3. Discussion and summary

First, we discuss durations of the various observed phases of the eruption. For the initial explosion at ∼15:46, we could not identify the N-shaped pulsation in ionospheric TEC which may appear ∼10 min later. As shown in the short period (17–33 s) seismic signals (Fig. 3(b)) possibly caused by the ground vibration in the continuous eruption, the Plinian eruption may have started at ∼16:01 UT and lasted for ∼2 h. After the termination of the Plinian eruption at ∼18 UT, long period signals (200–333 s) were observed until ∼19 UT both in the ionosphere (Fig. 3(a)) and on the ground (Fig. 3(b), the top curve). This would indicate the atmospheric free oscillation that continued even after the termination of the Plinian eruption, and decayed slowly in one hour.

The seismic signals from 16:25 UT to 18:00 UT showed peaks at 3.7 mHz, 4.8 mHz, 5.7 mHz and 6.8 mHz, suggesting that the lithosphere–atmosphere coupling also occurred along with the ionosphere–atmosphere coupling. The oscillations of TEC started at ∼16:25 UT, ∼20 min after the start of the Plinian eruption at ∼16:01. This time lag would reflect the time for the growth of the lower atmospheric oscillation to reach the ionospheric F layer (∼300 km). The Plinian eruption ended by ∼18 UT, however the ionospheric and lower atmospheric oscillations continued until ∼19:00 UT due to relatively large quality factor (Q). Atmospheric quality factor of 3.7 and 4.6 mHz are about 150 and 20, respectively (Rolland et al., 2011), and these Qs are high enough for the atmospheric free oscillation to continue by 1 h without further excitations.

Here we studied ionospheric signatures made by the eruption of the Kelud volcano on 13 February 2014, with regional networks of continuous GNSS receivers. This study gives the first detailed report of spatial distribution and time evolution of ionospheric disturbances by a Plinian eruption. First, the Plinian eruption would have caused atmospheric turbulences in its plume. The turbulence itself had broad frequency spectrum, and standing waves or acoustic fundamental and overtone modes trapped in the lower atmosphere were excited. Then, some part of the energy of these standing waves would have leaked into the ionosphere and lithosphere, resulting in spectral peaks in TEC and seismograms. This Plinian eruption that drove the multi-sphere oscillations ended at ∼18 UT, and only low frequency oscillation continued for one more hour in the ionosphere and lower atmosphere.

This study can be summarized as follows.

(1) With the GNSS-TEC technique, we observed ionospheric oscillations forced by lower atmospheric natural vibration after the start of the 2014 February Plinian eruption of the Kelud volcano, Indonesia. The Plinian eruption lasted from ∼16:01 UT to ∼18:00 UT while the TEC oscillation lasted from ∼16:25 to ∼19:00 UT. The TEC oscillations showed frequency peaks at 3.7 mHz and 4.8 mHz.

(2) Spectra of the seismic records showed peaks of a series of atmospheric acoustic modes, 3.7 mHz and 4.8 mHz, and two higher modes. These frequency peaks suggest that the harmonic ground motions are excited by the coupling between the solid Earth and the lower atmosphere.

Acknowledgements

We would like to thank to Geospatial Information Agency (Indonesia) for providing GNSS data within limited term. IGS data are available from the web (ftp://garner.ucsd.edu/). GEOFON and GSN data are available from GFZ and IRIS data management centers, respectively.

Appendix A. Supplementary material

Supplementary material related to this article can be found online at http://dx.doi.org/10.1016/j.epsl.2015.11.029.

References

Bilitza, D., McKinnell, L.-A., Reinisch, B., Fuller-Rowell, T., 2011. The international reference ionosphere today and in the future. J. Geod. 85 (12), 909–920. http://link.springer.com/10.1007/s00190-010-0427-x.

Choosakul, N., Saito, A., Iyemori, T., Hashizume, M., 2009. Excitation of 4-min periodic ionospheric variations following the great Sumatra–Andaman earthquake in 2004. J. Geophys. Res. 114 (A10), A10313. http://doi.wiley.com/10.1029/2008JA013915.

Corentin, C., Benoit, T., Milton, G., Alexis, L.P., Pierrick, M., 2015. On the use of remote infrasound and seismic stations to constrain the eruptive sequence and intensity for the 2014 Kelud eruption. Geophys. Res. Lett.

Dautermann, T., Calais, E., Lognonné, P., Mattioli, G.S., 2009a. Lithosphere–atmosphere–ionosphere coupling after the 2003 explosive eruption of the Soufriere Hills Volcano, Montserrat. Geophys. J. Int. 179 (3), 1537–1546. http://gji.oxfordjournals.org/cgi/doi/10.1111/j.1365-246X.2009.04390.x.

Dautermann, T., Calais, E., Mattioli, G.S., 2009b. Global positioning system detection and energy estimation of the ionospheric wave caused by the 13 July 2003 explosion of the Soufrière Hills Volcano, Montserrat. J. Geophys. Res. 114 (B2), B02202. http://doi.wiley.com/10.1029/2008JB005722.

Dziewonski, Adam M., Anderson, Don L., 1981. Preliminary reference Earth model. Phys. Earth Planet. Inter. (ISSN 0031-9201) 25 (4), 297–356. http://dx.doi.org/10.1016/0031-9201(81)90046-7.

Heki, K., 2006. Explosion energy of the 2004 eruption of the Asama Volcano, central Japan, inferred from ionospheric disturbances. Geophys. Res. Lett. 33 (14), L14303. http://doi.wiley.com/10.1029/2006GL026249.

Kanamori, H., Mori, J., 1992. Harmonic excitation of mantle Rayleigh waves by the 1991 eruption of Mount Pinatubo, Philippines. Geophys. Res. Lett. 19 (7), 721–724. http://onlinelibrary.wiley.com/doi/10.1029/92GL00258/full.

Kanamori, H., Mori, J., Harkrider, D., 1994. Excitation of atmospheric oscillations by volcanic eruptions. J. Geophys. Res., Solid Earth 99, 947–961. http://onlinelibrary.wiley.com/doi/10.1029/94JB01475/full.

Lognonné, P., Clevede, E., Kanamori, H., 1998. Computation of seismograms and atmospheric oscillations by normal-mode summation for a spherical earth model with realistic atmosphere. Geophys. J. Int. 135, 388–406. http://onlinelibrary.wiley.com/doi/10.1046/j.1365-246X.1998.00665.x/full.

Nishioka, M., Tsugawa, T., Kubota, M., Ishii, M., 2013. Concentric waves and short-period oscillations observed in the ionosphere after the 2013 Moore EF5 tornado. Geophys. Res. Lett. 40 (21), 5581–5586. http://doi.wiley.com/10.1002/2013GL057963.

Rolland, L.M., Lognonn, P., Astafyeva, E., Kherani, E.A., 2011. The resonant response of the ionosphere imaged after the 2011 off the Pacific coast of Tohoku Earthquake. Earth Planets Space 63 (7), 853–857. http://www.terrapub.co.jp/journals/EPS/abstract/6307/63070853.html.

Saito, A., Tsugawa, T., Otsuka, Y., Nishioka, M., Iyemori, T., Matsumura, M., Saito, S., Chen, C.H., Goi, Y., Choosakul, N., 2011. Acoustic resonance and plasma depletion detected by GPS total electron content observation after the 2011 off the Pacific coast of Tohoku Earthquake. Earth Planets Space 63 (7), 863–867. http://link.springer.com/10.5047/eps.2011.06.034.

Sulaksana, N., Sukiyah, E., Sudradjat, A., Syafri, I., 2014. The crater configuration of Kelud volcano, East Java, Indonesia after the 2014 eruption. Int. J. Sci. Res. 3 (3), 419–422. http://www.ijsr.net/archive/v3i3/MDIwMTMxMTQx.pdf.

Watada, S., Kanamori, H., 2010. Acoustic resonant oscillations between the atmosphere and the solid earth during the 1991 Mt. Pinatubo eruption. J. Geophys. Res. 115 (B12), B12319. http://doi.wiley.com/10.1029/2010JB007747.

Widmer, R., Zürn, W., 1992. Bichromatic excitation of long-period Rayleigh and air waves by the Mount Pinatubo and El Chichon volcanic eruptions. Geophys. Res. Lett. 19 (8), 765–768. http://onlinelibrary.wiley.com/doi/10.1029/92GL00685/full.